

## Regular Article

# Performance Analysis of MIMO Full-Duplex NOMA Networks with Max-Min Relay Selection for Short-Packet Communications

Do Phuong Nhung<sup>1</sup>, Nguyen Van Son<sup>1</sup>, Pham Thanh Hiep<sup>2</sup>, Hai-Nam Le<sup>3,\*</sup>

<sup>1</sup> Faculty of Electrics and Electronics, Hanoi Open University, B101 Nguyen Hien, Ha Noi, Viet Nam

<sup>2</sup> Advanced Wireless Communications Group, Le Quy Don Technical University, 236 Hoang Quoc Viet, Ha Noi, Viet Nam

<sup>3</sup> Institute of System Integration, Le Quy Don Technical University, 236 Hoang Quoc Viet, Ha Noi, Viet Nam

Correspondence: Hai-Nam Le, namlh@lqdtu.edu.vn

Communication: received 09 July 2025, revised 01 September 2025, accepted 10 September 2025

Online publication: 13 September 2025, Digital Object Identifier: 10.21553/rev-jec.412

**Abstract**– This paper investigates the performance of a multiple-input multiple-output (MIMO) non-orthogonal multiple access (NOMA) network, enhanced by a pool of full-duplex (FD) relays, for short-packet communications (SPC). We propose a combined framework where the source and destinations are equipped with multiple antennas, and a max-min relay selection criterion is employed to choose the best relay among multiple candidates. This criterion maximizes the end-to-end link quality by selecting the relay that offers the best bottleneck signal-to-interference-plus-noise ratio (SINR). We derive novel, exact analytical expressions for the average block error rate (BLER) for two NOMA users, meticulously accounting for the joint effects of MIMO diversity, relay selection diversity, residual self-interference (RSI) at the FD relay, and imperfect successive interference cancellation (SIC). To facilitate computation, we also provide a highly accurate closed-form approximation of the BLER using Gauss-Chebyshev quadrature. The analysis reveals that the max-min selection strategy effectively overcomes the performance bottleneck of simpler selection schemes, ensuring that the system's diversity order scales with the number of available relays. Numerical results, validated by Monte Carlo simulations, demonstrate the significant reliability gains achieved by the proposed framework. The findings offer crucial insights into the interplay between key system parameters, providing a comprehensive guide for designing robust ultra-reliable low-latency communication (URLLC) systems.

**Keywords**– Short-Packet Communication (SPC), NOMA, MIMO, Full-Duplex (FD), Relay Selection, Max-Min Criterion, Block Error Rate (BLER), URLLC.

## 1 INTRODUCTION

Ultra-reliable and low-latency communication (URLLC) constitutes a critical service class in 5G and future wireless networks, underpinning transformative applications like autonomous systems and tactile internet [1, 2]. The stringent demands of URLLC necessitate the use of short-packet communications (SPC), where data is transmitted in small blocks. The finite block-length nature of SPC, as characterized by Polyanskiy *et al.* [3], introduces a fundamental trade-off between latency, reliability, and data rate, making the block error rate (BLER) a primary performance metric [4].

To meet the dual demands of high spectral efficiency and massive connectivity, non-orthogonal multiple access (NOMA) has been identified as a key technology [5, 6]. Concurrently, multiple-input multiple-output (MIMO) techniques are indispensable for combating fading and enhancing reliability through spatial diversity. The synergy of MIMO and NOMA has been explored in [7, 8], but often in point-to-point or simple relaying scenarios. Furthermore, full-duplex (FD) relaying promises to double the spectral efficiency by enabling simultaneous transmission and reception [9, 10], though it introduces the challenge of residual self-interference (RSI) [11]. The performance of FD-NOMA systems with SPC has been studied, for instance,

in [12] and [13], but typically for a fixed relay with multiple antennas.

In practical deployments, cooperative relaying is vital for coverage extension and improving link reliability [14, 15]. The integration of NOMA into cooperative systems has been extensively studied to leverage both spatial diversity and improved spectral efficiency. Early works such as [16] laid the groundwork for cooperative NOMA, while subsequent studies analyzed its performance with different relaying protocols, such as amplify-and-forward (AF) in [17, 18] demonstrating significant gains over traditional OMA-based relaying.

To maximize these cooperative gains in multi-relay scenarios, relay selection offers a low-complexity method to exploit user diversity. The problem of relay selection in NOMA systems has been an active area of research. For instance, [19], [20], and [21] investigate various relay selection strategies to optimize the performance of different NOMA users, while [22] considers user scheduling in conjunction with relaying. However, these studies often focus on half-duplex systems and do not consider the implications of short-packet communications.

The performance of MIMO FD relay systems has been analyzed in works like [23], but the synergy of these advanced techniques, i.e., cooperative NOMA, FD relaying, and robust relay selection, under the stringent

constraints of URLLC, where fundamental limits are different from the infinite blocklength regime [24], remains an under-explored area.

While the individual benefits of MIMO, NOMA, and FD relaying are well-documented, their synergistic operation in the context of URLLC presents unique challenges and opportunities. Simple relay selection schemes, often based on single-hop metrics [25], can create performance bottlenecks, limiting the end-to-end reliability crucial for URLLC. The application of a more robust criterion like max-min selection [26, 27], which optimizes the entire two-hop path, to a comprehensive MIMO-NOMA FD system operating with short packets remains an open and important research area. This paper aims to bridge this gap by providing a rigorous analysis of how this powerful combination impacts the system's BLER, a key metric for URLLC.

This paper bridges this gap by developing and analyzing a holistic framework that combines MIMO, NOMA, FD relaying, and a max-min relay selection strategy for SPC. We aim to provide a rigorous analysis of how this powerful combination impacts the system's BLER. The main contributions are:

- We propose and analyze a holistic framework combining multi-antenna nodes, power-domain NOMA, full-duplex relaying, and a robust max-min relay selection strategy, specifically tailored for short-packet communications. This comprehensive model captures the complex interplay between spatial diversity, user diversity, and interference management under finite blocklength constraints.
- We derive novel and exact analytical expressions for the end-to-end SINR cumulative distribution function (CDF) under this advanced selection scheme, which forms the basis for our BLER analysis.
- We provide a detailed derivation of the average BLER for each NOMA user, and further propose a highly accurate closed-form approximation using Gauss-Chebyshev quadrature to make the results more tractable.
- We demonstrate through analysis and numerical results that the max-min selection scheme effectively leverages both user and spatial diversity, leading to significant performance improvements as the number of relays and antennas increases.

The paper is structured as follows. Section 2 details the system model and the max-min selection protocol. Section 3 presents the rigorous BLER analysis. Section 4 discusses the numerical results, and Section 5 concludes the paper.

## 2 SYSTEM MODEL

### 2.1 Network and Channel Model

As described in Figure 1, we consider a downlink cooperative NOMA network where a source (S) communicates with a far user ( $D_1$ ) and a near user ( $D_2$ ) via one selected relay from a set of  $K$  potential FD relays  $\{R_1, \dots, R_K\}$ . S,  $D_1$ , and  $D_2$  are equipped with

$N_S$ ,  $N_1$ , and  $N_2$  antennas, respectively. Each relay  $R_k$  has a single transmit and a single receive antenna operating in FD mode. Direct links from S to users are assumed to be unavailable due to obstacles such as tall buildings, trees, hills...

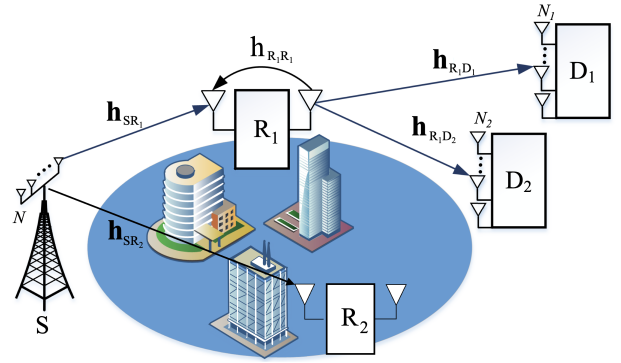


Figure 1. Network model of MIMO NOMA FD SPC with max-min relay selection from a set of  $K$  potential relays ( $K = 2$  is shown for illustration).

All channels are modeled as independent, quasi-static block fading. The channel vector between a multi-antenna node A and a single-antenna node B is denoted by  $\mathbf{h}_{AB}$ . The channel entries are assumed to follow a Nakagami- $m$  distribution. The squared norm of the channel vector after applying Maximal-Ratio Transmission (MRT) or Maximal-Ratio Combining (MRC), e.g.,  $G_{SR_k} = \|\mathbf{h}_{SR_k}\|^2$ , follows a Gamma distribution with shape parameter  $N_S m$  and scale parameter  $\Omega_{SR}/m$ , where  $\Omega_{SR}$  is the average channel power gain per antenna [28]. It is important to note that this work employs MRT/MRC beamforming, which utilizes all available antennas at the source and destinations to maximize the array gain. This is distinct from antenna selection schemes, where only a subset of antennas is activated. The RSI channel gain at relay  $R_k$ ,  $G_{R_k R_k} = |h_{R_k R_k}|^2$ , is modeled as an exponential random variable with mean  $\lambda_{RR}$ .

### 2.2 Signal Transmission and SINR Expressions

The transmission follows a two-hop, decode-and-forward (DF) protocol.

**2.2.1 First Hop ( $S \rightarrow R_k$ ):** S transmits the superimposed signal  $x_s = \sqrt{\alpha_1 P_S} s_1 + \sqrt{\alpha_2 P_S} s_2$ , where  $s_1$  and  $s_2$  are messages for  $D_1$  and  $D_2$ .  $P_S$  is the transmit power at S, and  $\alpha_1, \alpha_2$  are power allocation coefficients with  $\alpha_1 + \alpha_2 = 1$ . To serve the far user  $D_1$  with higher reliability, we set  $\alpha_1 > \alpha_2$ . The received signal at any relay  $R_k$  is

$$y_{R_k} = \mathbf{h}_{SR_k}^T \mathbf{w}_S x_s + h_{R_k R_k} \sqrt{\zeta P_R} x_{r,k} + n_{R_k}, \quad (1)$$

where  $\mathbf{w}_S$  is the MRT beamforming vector,  $P_R$  is the relay transmit power,  $\zeta$  is the RSI coefficient, and  $x_{r,k}$  is the signal transmitted by  $R_k$ . Following the successive interference cancellation (SIC) principle, relay  $R_k$  decodes  $s_1$  first while considering  $s_2$  as interference. The SINR for decoding  $s_1$  is given by

$$\gamma_{R_k \rightarrow s_1} = \frac{\alpha_1 P_S G_{SR_k}}{\alpha_2 P_S G_{SR_k} + \zeta P_R G_{R_k R_k} + \sigma^2}. \quad (2)$$

After detecting  $s_1$ , the relay  $R_k$  subtracts  $s_1$  from its received signal and decodes  $s_2$ . The SINR for decoding  $s_2$  with the imperfect SIC coefficient  $\kappa_1$ , is represented as

$$\gamma_{R_k \rightarrow s_2} = \frac{\alpha_2 P_S G_{SR_k}}{\kappa_1 \alpha_1 P_S G_{SR_k} + \xi P_R G_{R_k R_k} + \sigma^2}. \quad (3)$$

2.2.2 *Second Hop* ( $R_k \rightarrow D_i$ ): At  $D_1$  (far user), it decodes its own signal  $s_1$  directly; therefore, the SINR to decode  $s_1$  is depicted as follows

$$\gamma_{D_1,k} = \frac{\alpha_1 P_R G_{R_k D_1}}{\alpha_2 P_R G_{R_k D_1} + \sigma^2}. \quad (4)$$

At  $D_2$  (near user), similar to relay, it first decodes  $s_1$  while considering  $s_2$  as interference, and then decodes  $s_2$ . The decode process at  $D_2$  is assumed to be an imperfect SIC with coefficient  $\kappa_2$ , decodes  $s_2$ . The respective SINRs of  $s_1$  and  $s_2$  are represented as

$$\gamma_{D_2 \rightarrow s_1,k} = \frac{\alpha_1 P_R G_{R_k D_2}}{\alpha_2 P_R G_{R_k D_2} + \sigma^2}, \quad (5)$$

$$\gamma_{D_2,k} = \frac{\alpha_2 P_R G_{R_k D_2}}{\kappa_2 \alpha_1 P_R G_{R_k D_2} + \sigma^2}. \quad (6)$$

### 2.3 Max-Min Relay Selection Criterion

To optimize end-to-end reliability, the system selects the relay that maximizes the weakest link in the communication path. The end-to-end SINR for user  $D_i$  through relay  $R_k$  is limited by the minimum of the SINRs of all necessary decoding steps. The effective end-to-end SINR for  $D_1$  and  $D_2$  are, respectively.

$$\gamma_{e2e,1} = \max_{k \in \{1, \dots, K\}} \{ \min(\gamma_{R_k \rightarrow s_1}, \gamma_{D_1,k}) \}, \quad (7)$$

$$\gamma_{e2e,2} = \max_{k \in \{1, \dots, K\}} \{ \min(\gamma_{R_k \rightarrow s_1}, \gamma_{R_k \rightarrow s_2}, \gamma_{D_2 \rightarrow s_1,k}, \gamma_{D_2,k}) \}. \quad (8)$$

The practical implementation of this selection criterion is described in Algorithm 1. For analytical purposes, we assume the selection is performed to optimize each user's link independently, based on perfect and instantaneously available channel state information (CSI) at the source or a central controller.

**Algorithm 1** Max-Min Relay Selection Algorithm (for User  $D_1$ )

- 
- 1: **Input:** Channel gains  $\{G_{SR_k}, G_{R_k D_1}, G_{R_k R_k}\}_{k=1}^K$ .
  - 2: **Output:** Index of the best relay,  $k^*$ .
  - 3: Initialize  $\gamma_{max} \leftarrow -1$ ,  $k^* \leftarrow 0$ .
  - 4: **for**  $k = 1$  to  $K$  **do**
  - 5:   Calculate first-hop SINR:  $\gamma_{R_k \rightarrow s_1}$ .
  - 6:   Calculate second-hop SINR:  $\gamma_{D_1,k}$ .
  - 7:   Calculate path bottleneck SINR:  $\gamma_{path,k} \leftarrow \min(\gamma_{R_k \rightarrow s_1}, \gamma_{D_1,k})$ .
  - 8:   **if**  $\gamma_{path,k} > \gamma_{max}$  **then**
  - 9:      $\gamma_{max} \leftarrow \gamma_{path,k}$ .
  - 10:     $k^* \leftarrow k$ .
  - 11:   **end if**
  - 12: **end for**
  - 13: **return**  $k^*$ .
- 

## 2.4 Practical Implementation Aspects

The practical implementation of the max-min relay selection scheme requires a centralized entity, such as the source S or a base station controller, to manage the selection process. This process involves three main steps: 1) Channel Estimation: Each node estimates its relevant channel state information (CSI), e.g., via pilot signals. 2) CSI Feedback: The relays and destination users feed their estimated CSI back to the central controller. This step introduces overhead and is subject to delay and quantization errors in a practical system. 3) Relay Selection: The controller calculates the end-to-end bottleneck SINR for each of the  $K$  potential paths and selects the relay that maximizes this value. The index of the chosen relay is then broadcast to the network.

## 3 BLER PERFORMANCE ANALYSIS

### 3.1 Fundamentals of BLER in SPC

To begin the analysis, we first establish the fundamental relationship between the instantaneous SINR,  $\gamma$ , and the block error rate (BLER),  $\varepsilon(\gamma)$ , in the finite blocklength regime. As established by Polyanskiy et al. in [3], this relationship is not a simple step function but can be tightly approximated by the Gaussian Q-function, which captures the probabilistic nature of decoding errors for short data packets. For a given blocklength  $\mathcal{L}$  and  $b$  information bits, the transmission rate is  $R = b/\mathcal{L}$ . The instantaneous BLER,  $\varepsilon$ , for a given SINR  $\gamma$  can be tightly approximated as

$$\varepsilon(\gamma) \approx Q\left(\frac{\ln(1+\gamma) - R \ln 2}{\sqrt{V(\gamma)/\mathcal{L}}}\right), \quad (9)$$

where  $Q(x) = \frac{1}{\sqrt{2\pi}} \int_x^\infty e^{-t^2/2} dt$  is the Gaussian Q-function and  $V(\gamma) = 1 - (1+\gamma)^{-2}$  is the channel dispersion, representing the stochastic variability of the channel.

While Equation (9) provides the instantaneous BLER, evaluating the average BLER,  $\bar{\varepsilon} = \mathbb{E}_\gamma[\varepsilon(\gamma)]$ , requires integrating this expression over the probability distribution of the end-to-end SINR,  $\gamma$ . This integral is often intractable. To overcome this, we employ a highly accurate linear approximation of the Q-function, which transforms the problem into integrating the CDF of the SINR over a small interval [13, 29]. This leads to the following integral form

$$\bar{\varepsilon} \approx \chi \int_{\rho_L}^{\rho_H} F_\gamma(x) dx, \quad (10)$$

where  $F_\gamma(x)$  is the CDF of the end-to-end SINR  $\gamma$ . The parameters in this approximation are defined for each user  $i \in \{1, 2\}$  as follows:

- $R_i = b_i/\mathcal{L}_i$ : The transmission rate for user  $i$ .
- $\tau_i = 2^{R_i} - 1$ : The required SINR to achieve rate  $R_i$  in the infinite blocklength regime (Shannon capacity). This serves as the central point for the linear approximation.
- $V(\tau_i) = 1 - (1 + \tau_i)^{-2}$ : The channel dispersion evaluated at the SINR threshold.

- $\chi_i = \sqrt{\mathcal{L}_i/(2\pi V(\tau_i))}$ : A parameter representing the steepness of the BLER curve. A larger  $\chi_i$  indicates a sharper transition from unreliable to reliable communication.
- $\rho_{Li} = \tau_i - 1/(2\chi_i)$  and  $\rho_{Hi} = \tau_i + 1/(2\chi_i)$ : The lower and upper bounds of the integration, defining the effective region where the BLER transitions from 1 to 0.

### 3.2 End-to-End SINR Distribution

The core of the analysis is to derive the CDF of the end-to-end SINR,  $F_{\gamma_{e2e}}(x)$ . The derivation follows a bottom-up approach.

**3.2.1 CDF of a Single MIMO Link:** The channel power gain  $G$  after MRC/MRT over  $N$  antennas with Nakagami- $m$  fading follows a Gamma distribution. Its CDF is given by [30]

$$F_G(g; N, m, \Omega) = \frac{\gamma(Nm, mg/\Omega)}{\Gamma(Nm)}, \quad (11)$$

where  $\gamma(\cdot, \cdot)$  is the lower incomplete gamma function.

**3.2.2 CDF of SINR for an Individual Hop:** The CDF of the SINR for each hop can be expressed in terms of  $F_G(\cdot)$ . For the second hop at  $D_1$  via relay  $k$ , the CDF of the SINR is represented by

$$F_{\gamma_{D1,k}}(x) = F_G\left(\frac{x}{\rho_R(\alpha_1 - \alpha_2 x)}; N_1, m, \Omega_{RD1}\right), \quad (12)$$

where  $\rho_R = P_R/\sigma^2$ . For the first hop, the CDF is found by integrating over the RSI channel gain.

$$F_{\gamma_{Rk \rightarrow s1}}(x) = \int_0^\infty F_G(g_{req}; N_S, m, \Omega_{SR}) \frac{e^{-g_{rr}/\lambda_{RR}}}{\lambda_{RR}} dg_{rr}, \quad (13)$$

where  $g_{req} = \frac{x(\xi\rho_R g_{rr} + 1)}{(\rho_S(\alpha_1 - \alpha_2 x))}$  and  $\rho_S = P_S/\sigma^2$ .

**3.2.3 CDF for a Single End-to-End Path and after Selection for User D1:** The CDF for a single path through relay  $k$  for user  $D_1$  is  $F_{path,1,k}(x) = 1 - (1 - F_{\gamma_{Rk \rightarrow s1}}(x))(1 - F_{\gamma_{D1,k}}(x))$ . After max-min selection over  $K$  relays, the final CDF is

$$F_{\gamma_{e2e,1}}(x) = [F_{path,1,k}(x)]^K. \quad (14)$$

### 3.3 Average BLER and Closed-Form Approximation for User D1

The integral in (10) is often difficult to solve in a simple closed form. Following the approach in [13], we can use the Gauss-Chebyshev quadrature rule to obtain a highly accurate closed-form approximation.

$$\int_{\rho_L}^{\rho_H} f(x) dx \approx \frac{\rho_H - \rho_L}{2} \sum_{j=1}^{N_p} w_j f(x_j), \quad (15)$$

where  $N_p$  is the number of quadrature points (a small value like 15-20 is often sufficient), and the weights  $w_j$

and evaluation points  $x_j$  are given by

$$y_j = \cos\left(\frac{(2j-1)\pi}{2N_p}\right), \quad (16)$$

$$x_j = \frac{\rho_H - \rho_L}{2} y_j + \frac{\rho_H + \rho_L}{2}, \quad (17)$$

$$w_j = \frac{\pi}{N_p} \sqrt{1 - y_j^2}. \quad (18)$$

**Proposition 1.** *The average BLER for user  $D_1$  can be accurately approximated in a closed form as*

$$\bar{\epsilon}_{D1} \approx \chi_1 \frac{\rho_{H1} - \rho_{L1}}{2} \sum_{j=1}^{N_p} w_j [F_{path,1,k}(x_j)]^K. \quad (19)$$

### 3.4 Average BLER and Closed-Form Approximation for User D2

Unlike the far user D1, the near user D2 must perform SIC. This means that for D2 to successfully decode its own message ( $s_2$ ), a chain of prior decoding events must succeed. Specifically, the selected relay  $R_k$  must first decode  $s_1$ , then  $s_2$ . Subsequently, D2 must also decode  $s_1$  to subtract it from the received signal before finally decoding  $s_2$ . A failure at any of these four stages results in an end-to-end error for D2.

Consequently, the effective end-to-end SINR for D2 is limited by the bottleneck of these four processes:  $\gamma_{e2e,2} = \max_k \{\min(\gamma_{Rk \rightarrow s1}, \gamma_{Rk \rightarrow s2}, \gamma_{D2 \rightarrow s1,k}, \gamma_{D2,k})\}$ . The CDF of the SINR for a single path through relay  $k$  is the probability that at least one of these SINRs is below a threshold  $x$ , given by

$$F_{path,2,k}(x) = 1 - \prod_{j=1}^4 (1 - F_{\gamma_j}(x)),$$

where  $\gamma_j$  represents the four respective SINR terms, whose individual CDFs can be derived similarly to the previous section. After max-min selection over  $K$  relays, the final CDF is  $F_{\gamma_{e2e,2}}(x) = [F_{path,2,k}(x)]^K$ . This leads to the final average BLER approximation for D2.

**Proposition 2.** *The average BLER for user  $D_2$  can be accurately approximated in a closed form as*

$$\bar{\epsilon}_{D2} \approx \chi_2 \frac{\rho_{H2} - \rho_{L2}}{2} \sum_{j=1}^{N_p} w_j [F_{path,2,k}(x_j)]^K. \quad (20)$$

## 4 NUMERICAL RESULTS AND DISCUSSION

In this section, we present numerical results to validate our analysis and illustrate the performance of the proposed scheme. For performance comparison, we include a baseline scheme referred to as ‘Simpler selection’. This method, often found in the literature, selects the relay that maximizes the channel gain of the first hop only (i.e.,  $\max_k G_{SRk}$ ), without considering the quality of the second hop to the destination. For simplicity and without loss of generality, the average channel power gains per antenna and the RSI channel gain are normalized to one, i.e.,  $\Omega_{SR} = \Omega_{RD1} = \lambda_{RR} = 1$ ,  $\Omega_{RD2} = 1.5$ . The noise variance is also

normalized,  $\sigma^2 = 1$ . The transmit power at the source and relays are assumed to be equal,  $P_S = P_R = P$ , thus the transmit signal-to-noise ratio (SNR) is defined as  $\rho = P/\sigma^2$ . Unless otherwise specified in the figures, the default system parameters are set as follows: number of antennas at each node  $N_S = N_1 = N_2 = N = 3$ , number of relays for selection  $K = 2$ , blocklength  $L = 256$ , number of information bits  $b_1 = b_2 = 256$ , Nakagami- $m$  fading parameter  $m = 3$ , power allocation coefficient for the far user  $\alpha_1 = 0.8$ , RSI coefficient  $\xi = 0.01$ , and imperfect SIC coefficients  $\kappa_1 = \kappa_2 = 0.01$ .

Figure 2 shows the BLER performance as a function of SNR for different numbers of antennas  $N$ . As expected, increasing  $N$  provides a significant performance improvement for both users. The steeper slope of the curves for larger  $N$  indicates a higher diversity order, which is a direct result of the spatial diversity gain from the MIMO configuration. This highlights the crucial role of multiple antennas in achieving the high reliability required for URLLC.

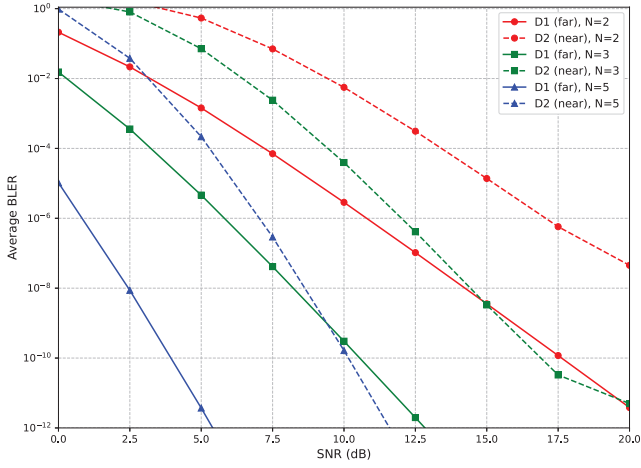


Figure 2. BLER vs. SNR for different numbers of antennas ( $N$ ), with  $K = 2$ .

Figure 3 illustrates the impact of the number of available relays  $K$  when using the max-min selection criterion compared to the simple selection scheme. The results clearly show that increasing  $K$  from 2 to 4 yields a substantial SNR gain. For instance, to achieve a BLER of  $10^{-10}$  for the far user  $D_1$ , the max-min selection scheme with  $K = 4$  requires approximately 10dB less SNR than the simple selection scheme. This confirms that the max-min selection strategy effectively leverages user diversity to combat fading and enhance reliability. The performance of the near user ( $D_2$ ) is notably high, achieving very low BLER at low SNRs, especially for  $K = 4$ . This is a direct consequence of the combined gains from the stronger channel inherent to the near user in NOMA, the spatial diversity from the MIMO configuration, and the user diversity provided by the max-min relay selection. This synergistic effect underscores the effectiveness of the proposed framework in achieving ultra-reliability. Note that some simulation markers are not visible as their BLER values fall below the plot's y-axis range.

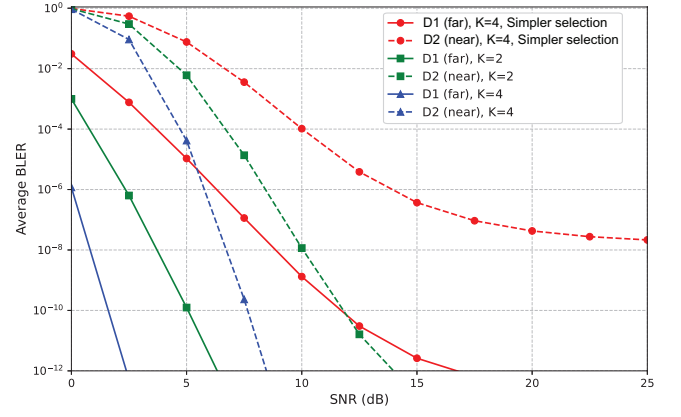


Figure 3. BLER vs. SNR for different numbers of relays ( $K$ ), with  $N = 3$ .

Figure 4 demonstrates the fundamental trade-off between latency (related to  $L$ ) and reliability. For a fixed SNR, a larger blocklength  $L$  allows for more powerful channel coding, thus reducing the BLER. Conversely, to meet a stringent BLER target with a shorter packet (smaller  $L$ ), a higher SNR is required.

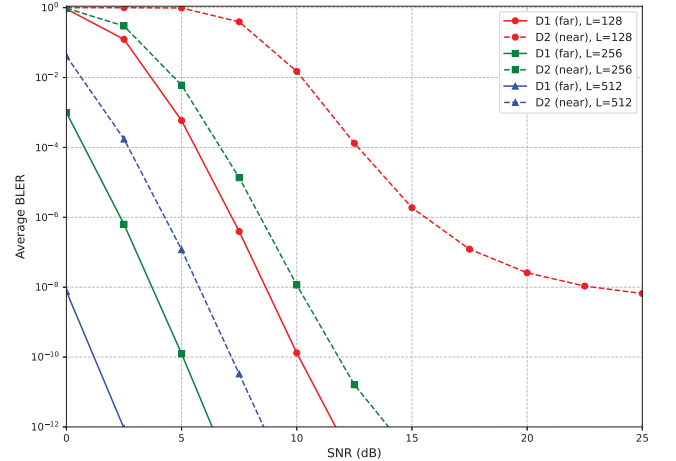


Figure 4. BLER vs. SNR for different blocklengths ( $L$ ), with  $N = 3, K = 2$ .

Figure 5 shows the BLER as a function of the number of transmitted bits  $b$  for different Nakagami- $m$  fading parameters. As  $b$  increases, the transmission rate  $R = b/L$  increases, raising the BLER. The figure also shows that a more benign channel environment (higher  $m$ ) drastically improves performance.

Figure 6 is now dedicated to analyzing the critical impact of the residual self-interference (RSI) coefficient,  $\xi$ , on the system's BLER performance. As RSI is the primary challenge in FD systems, this analysis is crucial for understanding practical limitations. The results clearly show that as  $\xi$  increases, the performance of both users degrades significantly. For a low RSI level ( $\xi = 0.001$ ), the system performance is excellent. However, for a higher RSI level ( $\xi = 0.15$ ), a prominent 'error floor' emerges for both users at high SNRs. This phenomenon occurs because, at high SNRs, the

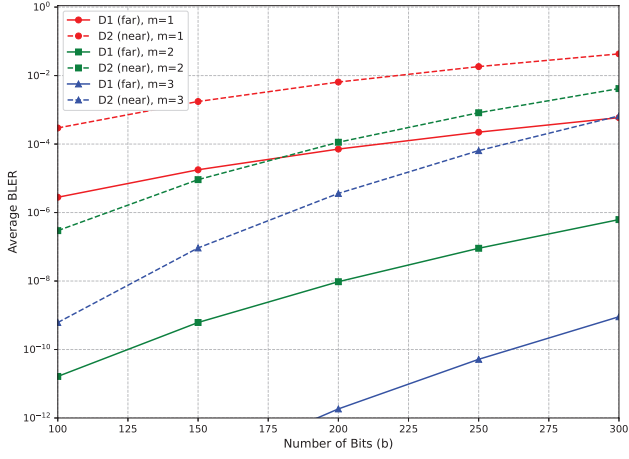


Figure 5. BLER vs. number of bits ( $b$ ) for different fading parameters ( $m$ ), with  $N = 2, K = 2, L = 256, \text{SNR} = 10\text{dB}$ .

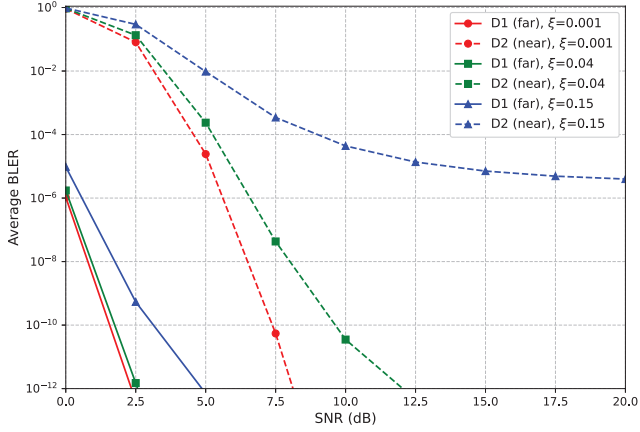


Figure 6. BLER vs. SNR for different RSI levels ( $\xi$ ), with  $K = 4, N = 3, L = 256$ .

system becomes interference-limited rather than noise-limited. The constant RSI power dominates the denominator of the SINR expression at the relay, creating a ceiling on the achievable SINR and, consequently, a floor on the BLER. This highlights the paramount importance of effective self-interference cancellation techniques to unlock the full potential of FD relaying in URLLC systems.

Figure 7 investigates the impact of power allocation and RSI. For the near user ( $D_2$ ), there is a clear optimal value of  $\alpha_1$  that minimizes its BLER, representing a trade-off between its own signal power and the interference from  $s_1$ . The BLER of the far user ( $D_1$ ) monotonically decreases as its allocated power  $\alpha_1$  increases. The plot also confirms that lower RSI (smaller  $\xi$ ) leads to significantly better performance.

Finally, Figure 8 shows the effect of imperfect SIC, represented by  $\kappa$ . The performance of the far user  $D_1$  is independent of  $\kappa$ . However, the BLER of the near user  $D_2$  degrades as  $\kappa$  increases. The case  $\kappa = 0$  represents perfect SIC and provides a lower bound on performance, highlighting the sensitivity of the NOMA near user to SIC quality.

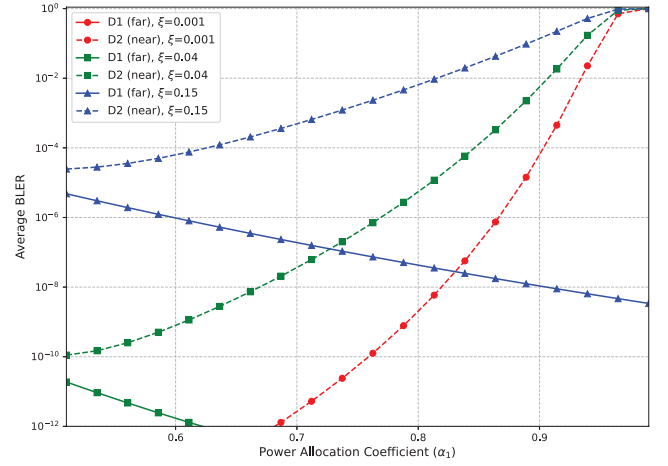


Figure 7. BLER vs. power allocation ( $\alpha_1$ ) for different RSI levels ( $\xi$ ), with  $N = 3, K = 2, L = 256, \text{SNR} = 10\text{dB}$ .

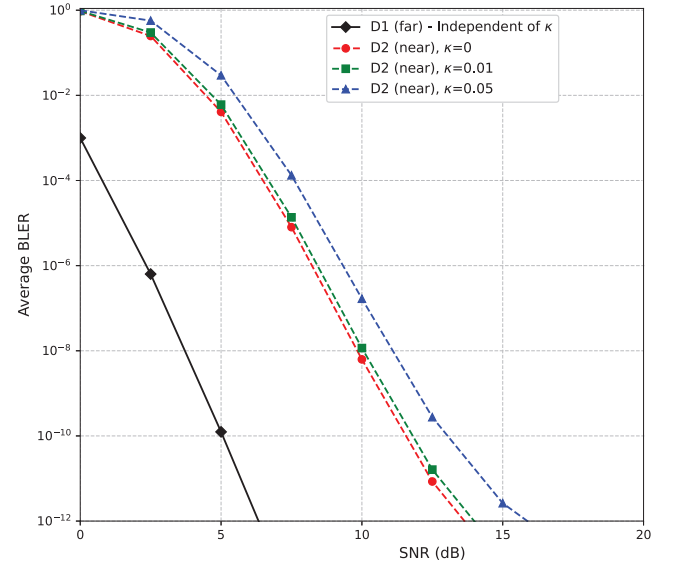


Figure 8. BLER vs. SNR for different SIC imperfection levels ( $\kappa$ ), with  $N = 3, K = 2$ .

## 5 CONCLUSION

This paper has provided a rigorous and comprehensive performance analysis for a sophisticated cooperative network combining MIMO, FD-NOMA, and a max-min relay selection strategy for short-packet communications. We derived novel, exact analytical expressions for the average BLER that capture the complex interactions between these advanced techniques. Our results unequivocally demonstrate that the synergy of multi-antenna processing and an intelligent max-min relay selection scheme can significantly boost system reliability compared to the traditional relay selection scheme. The analysis provides valuable, quantitative insights into the design trade-offs for URLLC systems. This work lays a strong theoretical foundation for the practical design and optimization of future-generation, high-reliability wireless networks.

## ACKNOWLEDGMENT

This work is supported by the Hanoi Open University, Vietnam, under the Grant No. MHN2024-01.01

## REFERENCES

- [1] P. Popovski, K. F. Trillingsgaard, O. Simeone, and G. Durisi, "5G wireless network slicing for eMBB, URLLC, and mMTC: A communication-theoretic view," *IEEE Access*, vol. 6, pp. 55765–55779, 2018.
- [2] C. She, C. Yang, and T. Q. Quek, "Radio resource management for ultra-reliable and low-latency communications," *IEEE Communications Magazine*, vol. 55, no. 6, pp. 72–78, 2017.
- [3] Y. Polyanskiy, H. V. Poor, and S. Verdú, "Channel coding rate in the finite blocklength regime," *IEEE Transactions on Information Theory*, vol. 56, no. 5, pp. 2307–2359, 2010.
- [4] G. Durisi, T. Koch, and P. Popovski, "Toward Massive, Ultrareliable, and Low-Latency Wireless Communication With Short Packets," *Proceedings of the IEEE*, vol. 104, no. 9, pp. 1711–1726, 2016.
- [5] Z. Ding, Y. Liu, J. Choi, Q. Sun, M. Elkashlan, I. Chih-Lin, and H. V. Poor, "Application of non-orthogonal multiple access in LTE and 5G networks," *IEEE Communications Magazine*, vol. 55, no. 2, pp. 185–191, 2017.
- [6] Z. Yang, Z. Ding, P. Fan, and N. Al-Dhahir, "A general power allocation scheme to guarantee quality of service in downlink and uplink NOMA systems," *IEEE Transactions on Wireless Communications*, vol. 15, no. 11, pp. 7244–7257, 2016.
- [7] D.-D. Tran, S. K. Sharma, S. Chatzinotas, I. Woungang, and B. Ottersten, "Short-packet communications for MIMO NOMA systems over Nakagami-m fading: BLER and minimum blocklength analysis," *IEEE Transactions on Vehicular Technology*, vol. 70, no. 4, pp. 3583–3598, 2021.
- [8] X. Sun, N. Yang, S. Yan, Z. Ding, D. W. K. Ng, C. Shen, and Z. Zhong, "Joint beamforming and power allocation in downlink NOMA multiuser MIMO networks," *IEEE Transactions on Wireless Communications*, vol. 17, no. 8, pp. 5367–5381, 2018.
- [9] T. Riihonen, S. Werner, and R. Wichman, "Mitigation of loopback self-interference in full-duplex MIMO relays," *IEEE Transactions on Signal Processing*, vol. 59, no. 12, pp. 5983–5993, 2011.
- [10] Z. Zhang, X. Chai, K. Long, A. V. Vasilakos, and L. Hanzo, "Full duplex techniques for 5G networks: self-interference cancellation, protocol design, and relay selection," *IEEE Communications Magazine*, vol. 53, no. 5, pp. 128–137, 2015.
- [11] T. Wang, H. Yang, and Q. Li, "Physical layer security for full duplex relay system," in *Proceedings of the 2023 IEEE International Symposium on Broadband Multimedia Systems and Broadcasting (BMSB)*. IEEE, 2023, pp. 1–3.
- [12] Y. Gu, H. Chen, Y. Li, and B. Vucetic, "Ultra-reliable short-packet communications: Half-duplex or full-duplex relaying?" *IEEE Wireless Communications Letters*, vol. 7, no. 3, pp. 348–351, 2017.
- [13] P. T. T. Huyen, B. Q. Bao, and N. T. Phuong, "Full-duplex relay non-orthogonal multiple access networks with short-packet communication: Block error rate and average achievable rate analysis," *Digital Signal Processing*, vol. 159, p. 104968, 2025.
- [14] J. N. Laneman, D. N. Tse, and G. W. Wornell, "Cooperative diversity in wireless networks: Efficient protocols and outage behavior," *IEEE Transactions on Information Theory*, vol. 50, no. 12, pp. 3062–3080, 2004.
- [15] Y. Liu, Z. Ding, M. Elkashlan, and H. V. Poor, "Cooperative non-orthogonal multiple access with simultaneous wireless information and power transfer," *IEEE Journal on Selected Areas in Communications*, vol. 34, no. 4, pp. 938–953, 2016.
- [16] Z. Ding, M. Peng, and H. V. Poor, "Cooperative non-orthogonal multiple access in 5G systems," *IEEE Communications Letters*, vol. 19, no. 8, pp. 1462–1465, 2015.
- [17] X. Liang, Y. Wu, D. W. K. Ng, Y. Zuo, S. Jin, and H. Zhu, "Outage performance for cooperative NOMA transmission with an AF relay," *IEEE Communications Letters*, vol. 21, no. 11, pp. 2428–2431, 2017.
- [18] X. Yan, H. Xiao, C.-X. Wang, and K. An, "Outage performance of NOMA-based hybrid satellite-terrestrial relay networks," *IEEE Wireless Communications Letters*, vol. 7, no. 4, pp. 538–541, 2018.
- [19] X. Yue, Y. Liu, S. Kang, A. Nallanathan, and Z. Ding, "Spatially Random Relay Selection for Full/Half-Duplex Cooperative NOMA Networks," *IEEE Transactions on Communications*, vol. 66, no. 8, pp. 3294–3308, 2018.
- [20] J. Ju, W. Duan, Q. Sun, S. Gao, and G. Zhang, "Performance analysis for cooperative NOMA with opportunistic relay selection," *IEEE Access*, vol. 7, pp. 131 488–131 500, 2019.
- [21] Z. Ding, H. Dai, and H. V. Poor, "Relay selection for cooperative NOMA," *IEEE Wireless Communications Letters*, vol. 5, no. 4, pp. 416–419, 2016.
- [22] D. Deng, L. Fan, X. Lei, W. Tan, and D. Xie, "Joint user and relay selection for cooperative noma networks," *IEEE Access*, vol. 5, pp. 20 220–20 227, 2017.
- [23] H. A. Suraweera, I. Krikidis, G. Zheng, C. Yuen, and P. J. Smith, "Low-Complexity End-to-End Performance Optimization in MIMO Full-Duplex Relay Systems," *IEEE Transactions on Wireless Communications*, vol. 13, no. 2, pp. 913–927, 2014.
- [24] J.-M. Gorce, P. Mary, D. Anade, and J.-M. Kélik, "Fundamental Limits of Non-Orthogonal Multiple Access (NOMA) for the Massive Gaussian Broadcast Channel in Finite Block-Length," *Sensors*, vol. 21, no. 3, p. 715, 2021.
- [25] A. Bletsas, A. Khisti, D. P. Reed, and A. Lippman, "A simple cooperative diversity method based on network path selection," *IEEE Journal on Selected Areas in Communications*, vol. 24, no. 3, pp. 659–672, 2006.
- [26] I. Krikidis, J. S. Thompson, S. McLaughlin, and N. Goertz, "Max-min relay selection for legacy amplify-and-forward systems with interference," *IEEE Transactions on Wireless Communications*, vol. 8, no. 6, pp. 3016–3027, 2009.
- [27] Y. Zhao, R. Adve, and T. J. Lim, "Improving amplify-and-forward relay networks: optimal power allocation versus selection," in *Proceedings of the 2006 IEEE international symposium on information theory*. IEEE, 2006, pp. 1234–1238.
- [28] Z. Chen, Z. Chi, Y. Li, and B. Vucetic, "Error performance of maximal-ratio combining with transmit antenna selection in flat Nakagami-m fading channels," *IEEE Transactions on Wireless Communications*, vol. 8, no. 1, pp. 424–431, 2009.
- [29] X. Lai, T. Wu, Q. Zhang, and J. Qin, "Average secure BLER analysis of NOMA downlink short-packet communication systems in flat Rayleigh fading channels," *IEEE Transactions on Wireless Communications*, vol. 20, no. 5, pp. 2948–2960, 2020.
- [30] M. Abramowitz and I. A. Stegun, *Handbook of mathematical functions: with formulas, graphs, and mathematical tables*. Courier Corporation, 1965, vol. 55.



**Do Phuong Nhung** Do Phuong Nhung graduated with a Master's degree in Electronic Engineering from Hanoi Open University, Hanoi, Vietnam. She is currently a Lecturer in the Department of Electrical and Electronics Engineering, Hanoi Open University. Her research areas include signal processing in 5G/6G systems and ML/AI applications in big data processing. Email: dpn-hung@hou.edu.vn



**Nguyen Van Son** Van Son Nguyen received the B.E. degree in electrical engineering and the M.S. degree in electronics and telecommunications engineering from Hanoi Open University, Hanoi, Vietnam. He is currently a Lecturer with the Faculty of Electrical and Electronic Engineering, Hanoi Open University. His research interests include signal processing in B5G/6G systems and ML/AI applications in big data processing. He can be contacted at e-mail: sonnv@hou.edu.vn.



**Hai-Nam Le** Dr. Hai-Nam Le received his Engineering and Master's Degrees in Electronic Engineering respectively in 1996 and 2001 from Le Quy Don Technical University in Hanoi; he received a Ph.D. (2006) in Communication Theory from the Moscow Institute of Physics and Technology. He has authored or co-authored more than 20 publications in journals and conference proceedings on circuit design, system architecture, multiple access control, and digital signal processing.



**Pham Thanh Hiep** Pham Thanh Hiep received a B.E. degree in Communications Engineering from the National Defense Academy, Japan, in 2005; and received the M.E. and Ph.D. degrees in Physics, Electrical and Computer Engineering from Yokohama National University, Japan, in 2009 and 2012, respectively. He worked as an associate researcher at Yokohama National University, Yokohama, Japan from 2012 to 2015. Now, he is a lecturer at Le Quy Don Technical University, Ha Noi, Vietnam. Prof. Hiep was a recipient of the best paper from The 25th National Conference on Electronics, Communications and Information Technology, and a co-recipient of the student best paper from The 2022 International Conference on Advanced Technologies for Communications. His research interests lie in the area of wireless communication technologies and signal processing. Further info on his homepage: <https://sites.google.com/view/phamthanhiep/home>